Z. Phys. Chem. **224** (2010) 1439–1473 / **DOI** 10.1524/zpch.2010.0046

Salt-in-Polymer Electrolytes for Lithium Ion Batteries Based on Organo-Functionalized Polyphosphazenes and Polysiloxanes

By Marina Burjanadze, Yunus Karatas[#], Nitin Kaskhedikar, Lutz M. Kogel, Sebastian Kloss, Ann-Christin Gentschev, Martin M. Hiller, Romek A. Müller, Raphael Stolina, Preeya Vettikuzha, and Hans-Dieter Wiemhöfer[*]

Institut für Anorganische und Analytische Chemie, Westfälische Wilhelms-Universität, Corrensstr. 28/30, 48149 Münster, Germany

(Received August 23, 2010; accepted in revised form October 6, 2010)

Polymer Electrolyte / Polyphosphazene / Polysiloxane / Ionic Conductivity / Electrochemistry / Polymer Synthesis

An overview is given on polymer electrolytes based on organo-functionalized polyphosphazenes and polysiloxanes. Chemical and electrochemical properties are discussed with respect to the synthesis, the choice of side groups and the goal of obtaining membranes and thin films that combine high ionic conductivity and mechanical stability. Electrochemical stability, concentration polarization and the role of transference numbers are discussed with respect to possible applications in lithium batteries. It is shown that the ionic conductivities of salt-in-polymer membranes without additives and plasticizers are limited to maximum conductivities around 10^{-4} S/cm. Nevertheless, a straightforward strategy based on additives can increase the conductivities to at least 10^{-3} S/cm and maybe further. In this context, the future role of polymers for safe, alternative electrolytes in lithium batteries will benefit from concepts based on polymeric gels, composites and hybrid materials. Presently developed polymer electrolytes with oligoether sidechains are electrochemically stable in the potential range 0–4.5 V (*vs.* Li/Li^+ reference).

1. Introduction

There are numerous reasons why polymer concepts are attractive for electrolytes and electrodes in lithium ion batteries. This was soon recognized when the first publications concentrating on polyethylene oxide (PEO) as the solvent had been released [1–4]. Not much later, the first publications appeared

[*] Corresponding author. E-mail: hdw@uni-muenster.de
[#] *Present address*: Ahi Evran Univ., Dept. Chem., 40200 Kirsehir, Turkey

on lithium salt containing polyphosphazenes as electrolytes which showed distinctly higher ionic conductivities as compared to linear PEO [5–7]. It has already been recognized at early stage that the much higher segmental mobility of these inorganic polymers with the third row element phosphorous was responsible for the improved results. This holds also for the polysiloxanes which tend to exhibit high segmental mobility in connection with a low glass transition temperature. Accordingly, analogous experiments with polysiloxane based polymer electrolytes were published not much later [8,9].

A considerable number of general overviews are available describing the developments in the general field of polymer electrolytes since then [10–14]. The advantages of polymeric solvents for battery electrolytes are evident. Liquid electrolytes are volatile and impose safety problems in current lithium ion batteries. It would be attractive to replace them by incombustible salt-in-polymer materials with no leakage problem. Cross-linked polymer electrolytes result in a safe separation of electrode components, prevent short-circuit in H.-D. Wiemhöfer and minimize the dissolution of electrode components. Furthermore, ion or even mixed conducting polymers may be applied as additives or binders in future electrode structures where they help to stabilize the network of active particles and, at the same time, support ion and/or electron transport within the three-dimensional electrode structures [15–17]. From a chemical standpoint, polymer properties are fixed by the monomers and their functional groups which determine polarity, degree of inter- and intramolecular interaction, mechanical stability and segmental mobility. In addition, different polymers can be combined in blends or copolymers or used as part of composite or hybrid systems offering a whealth of options to influence the properties. Chemical cross-linking can be used to stabilize the mechanical properties.

This overview focuses on the chemistry and electrochemistry of polyphosphazenes and polysiloxanes as host systems for dissolved salts. The emphasis lies on their use in ion conducting salt-in-polymer membranes, with the background of lithium ion batteries (although, apart from that, a series of proton conducting polyphosphazenes was synthesized and investigated, too, within this research [18–20]). This article compiles corresponding research results obtained within the SFB 458 which was devoted to the analysis of ion conduction and ion transport mechanisms in disordered materials. Recent trends and other work regarding ion conducting polyphosphazenes and polysiloxanes will be commented, too.

2. Polymer electrolytes with inorganic backbones

First of all, we discuss the influence of chemistry on the conductive properties of simple salt-in-polymer systems based on polyphosphazenes and polysiloxanes. The emphasis lies on the choice of grafted side chains and of the lithium

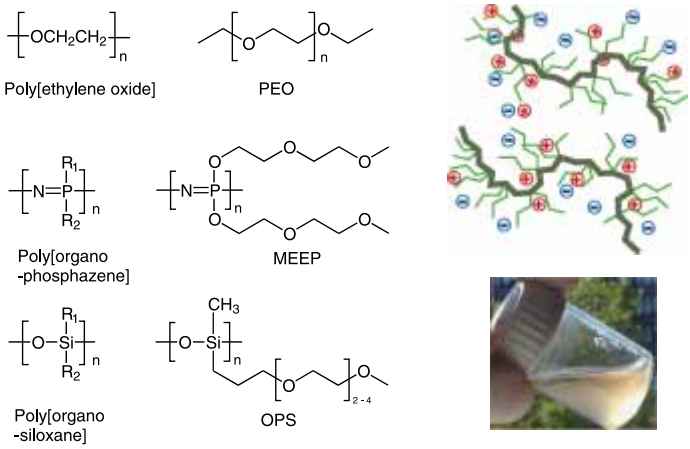

Scheme 1. Linear PEO and two polyether-grafted polymers with inorganic backbone are shown (graft copolymers are sometimes also termed comb polymers). The interaction with salt ions and also further properties depend on the choice of the side chains. The inorganic polymer backbones exhibit an exceptional segmental mobility. On the right above: illustration of the salt-in-polymer concept with a graft copolymer; on the right below: liquid OPS. Both, OPS and MEEP are viscous liquids due to an extremely low glass transition temperature (−54 and −83 °C, respectively).

salts. Extremely low T_g values lead to poor mechanical properties. Therefore, approaches to achieve better mechanical stabilities without depressing the ionic conductivity are an issue lateron.

2.1 Basic chemical approach to salt-in-polymer materials

Scheme 1 shows the basic monomeric units of these polymers with inorganic backbone as compared to the archetype of polymer electrolyte solvents, the linear polyethylene oxide (PEO). The main difference is that the hetero atoms Si and P, respectively, carry two sidegroups which can easily be modified by direct substitution or addition reactions with precursor polymers (so-called polymer analogous reactions), by ring opening polymerization of substituted cyclic phosphazenes or cyclic siloxanes, or by polymerization of differently substituted monomers [21,22]. The two substituents at a P or Si atom may be the same or may differ.

Polyphosphazenes and polysiloxanes, functionalized with varying organic sidechains at the phosphorous and silicon atoms, respectively, are the chemical background of this overview. They are frequently denoted as graft-copolymers, in particular if extended sidechains are used, or as comb polymers. The broad choice of sidegroups offers an enormous variability of properties and a straightforward approach to fine tune the physical and chemical properties. Hence, a particular feature of our work on polysiloxanes and polyphosphazenes was

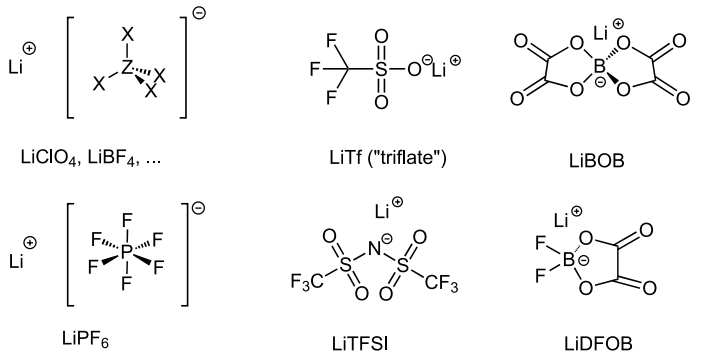

Scheme 2. Popular lithium salts as often used in polymer electrolytes.

to apply synthetic strategies for a flexible and optimized functionalization of polymers intended for ion conducting salt-in-polymer membranes.

The bonding angles of the inorganic backbones −P=N− and −Si−O− are less restricted as compared to carbon based chains. This is the reason for a high segmental mobility and rather low glass transition temperatures.

Mostly, short polyethylene oxide side chains (or: oligoethylene oxide) have been used in ion conducting polyphosphazenes and polysiloxanes. Examples are shown in Scheme 1. Therefore, in all such polymers, the main interaction occurs between the oxygen atoms of the polymer sidechains and the lithium ions whereas the anions remain loosely associated in the vicinity. Thus, the lithium ion mobility is lower than that of the anions, giving rise to a lower cation transference number [23–25].

A disadvantage of polyethylene oxide based polymer electrolytes is the low value of the relative permittivity as compared to the polar solvents of conventional liquid electrolytes used in lithium batteries. In order to achieve a high level of dissociation into cations and anions, the choice of the anions for the lithium salts is an important issue as will be demonstrated on various polymer electrolytes in the following. Single charged highly symmetric anions with low basicity are to be preferred. Larger anions that can delocalize the charge over a larger volume are even better. Scheme 2 shows some of the most most frequently used lithium salts in polymer based electrolytes. Note that $LiPF_6$ cannot be used in the context of polysiloxanes as formation of fluoride ions leads to degradation accompanied by formation of volatile SiF_4.

2.2 Polymer electrolytes based on polyphosphazenes

A great deal of the chemistry of organo-functionalized polyphosphazenes and of corresponding synthetic procedures has been investigated by H. A. Allcock and coworkers starting in the 70s [21]. A common, traditional way of polyphosphazene synthesis was based on the thermally initiated ring opening

Table 1. Synthetic routes to polyphosphazenes.

Synthetic route	Reactands/product data
Thermal ring opening Allcock *et al*. [29]	$N_3P_3Cl_6$ (250 °C), high M_n, broad PDI
Condensation polymerization De Jaeger *et al*. [30]	$Cl_3P{=}NP(O)Cl_2$, $M_n = 10^5$ g/mol, PDI = 1.5–3.0
Condensation polymerization Numerous investigators [31]	$PCl_5 + NH_4Cl$, medium M_n, very broad PDI
Living anionic polymerization Flindt *et al*. [32]	$(RO)_3P{=}NSiMe_3$, medium M_n, PDI = 1.3–2.4
Living cationic polymerization Manners, Allcock *et al*. [33,34]	$Cl_3P{=}NSiMe_3$, controlled M_n = (10^3–10^6 g/mol), narrow PDI

M_n – number average molar mass in g/mol (= molar mass); PDI – polydispersity index = quotient M_w/M_n of number-average and weight-average molar masses

polymerization of hexachloro-cyclotriphosphazene, *i.e.* $[NPCl_2]_3$. The latter is available in very good quality *via* reaction of PCl_5 and NH_4Cl.

Several other routes to polyphosphazenes are known, a compilation is given in Table 1 [21,26]. A particularly interesting method (last one in Table 1) was reported in 1997 consisting of a cationic living polymerization of phosphazene monomers with PCl_5 as chain growth initiator [27]. However, at the beginning, it was quite difficult to synthesize the monomeric phosphazene with the necessary purity according to the available procedures [28].

In 2002, a remarkable progress was achieved by Wang *et al.*, with a one pot synthesis of the phosphazene monomer $Cl_3P{=}NSi(CH_3)_3$ which is illustrated in Scheme 3 [35,36]. This route is characterized by a remarkably high yield and purity of the monomer which can be used directly and without isolation for a subsequent polymerization after addition of PCl_5 as initiator.

For the work on polyphosphazenes as presented in the following, the monomer synthesis of Scheme 3 was applied as the starting step towards the preparation of our polymeric precursor $(NPCl_2)_n$ [37,38]. The yield of the polymerization normally reached 80–90% of the monomer and the average molar mass was well controlled by the molar ratio PCl_5/phosphazene monomer [37,38]. Molar masses of 10^5–10^6 g/mol imposed no problem.

The freshly prepared precursor $(NPCl_2)_n$ acted as a source for numerous differently functionalized polyphosphazenes. All were obtained using the nucleophilic substitution reaction with corresponding alcohols and amines as illustrated in Scheme 4.

Scheme 5 shows a compilation of some substituents which have been applied in our experiments with ion conducting polyphosphazenes. With some bulky substituents, it is difficult to achieve a complete substitution of the chlor-

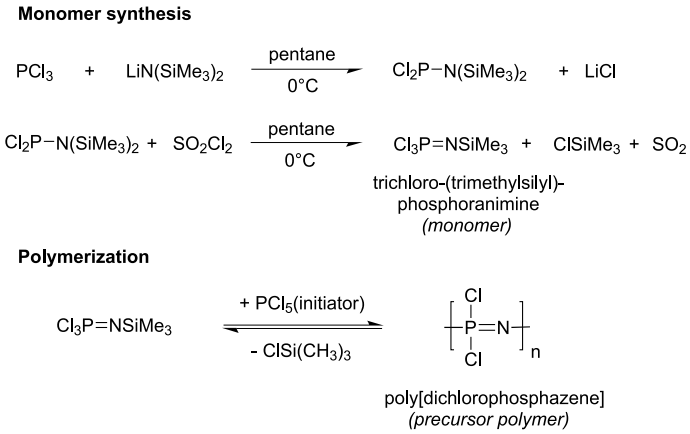

Scheme 3. Synthesis of the chlorinated polyphosphazene by the living polymerization route which is used as a versatile precursor for preparation of organo-functionalized polyphosphazenes [37,38]. The molar mass is controlled by the ratio of the monomer to the initiator PCl_5 (av. $M_n = 10^5$–10^6 g/mol [37]).

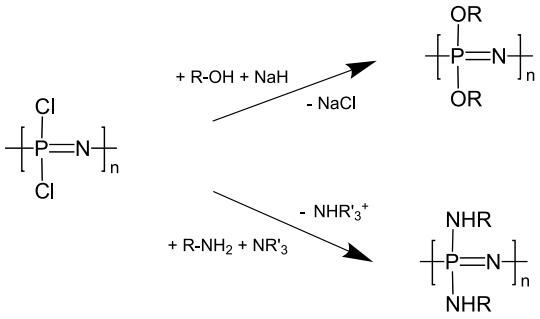

Scheme 4. Preparation of functionalized polyphosphazenes from the precursor polymer $(NPCl_2)_n$ by polymer substitution reactions from alcohols and amines (primary and secondary).

ine atoms in the precursor $(NPCl_2)_n$. This was observed for some secondary amines, long chain alcohols and branched side chains. In such cases, one has to complete the chlorine substitution in a second step by using small size primary amines or alcohols. This is the reason why the polyphosphazene, denoted as BMEAP in Scheme 5, was prepared with two kinds of amine side chains, a branched one and the linear $-NHCH_2CH_2CH_3$ (*cf*. Scheme 5).

Scheme 6 illustrates the variability and the great influence of the particular substitution pattern in polyphosphazenes on their physical properties. The polymers in Scheme 6 were synthesized with the aim to prepare and investigate proton conducting polyphosphazene membranes after introducing acidic sulfonate groups by a sulfonation of the aromatic rings [18]. The

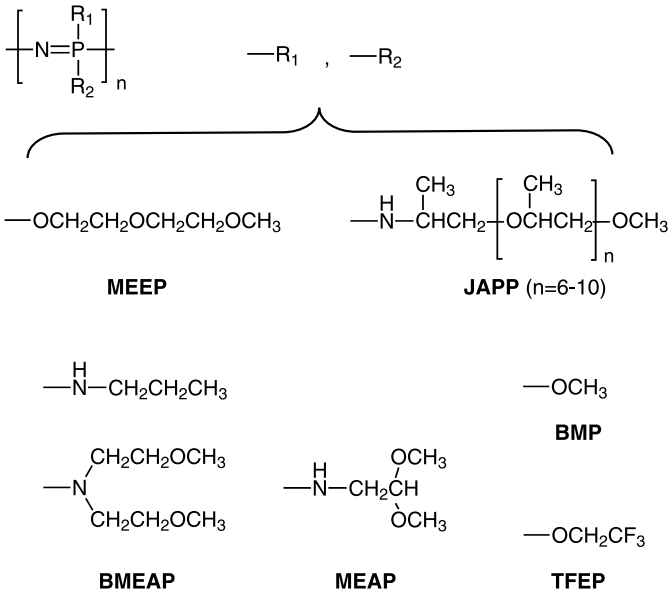

Scheme 5. Examples for substituents which were used to prepare functionalized polyphosphazenes for polymer electrolyte investigations with dissolved lithium salts; the abbreviations for the corresponding polyphosphazenes below the chemical formulas are used in the following text.

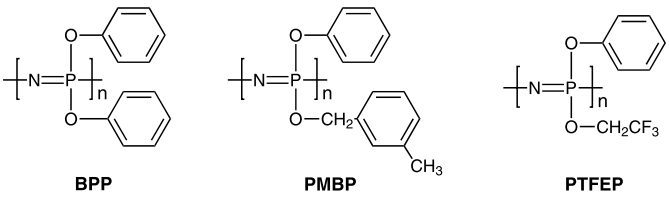

Scheme 6. Illustration of the variable physico-chemical properties of polyphosphazenes by changing or mixing the substituents [18,19]; the three polymer samples have average molecular weights around 10^5 g/mol.

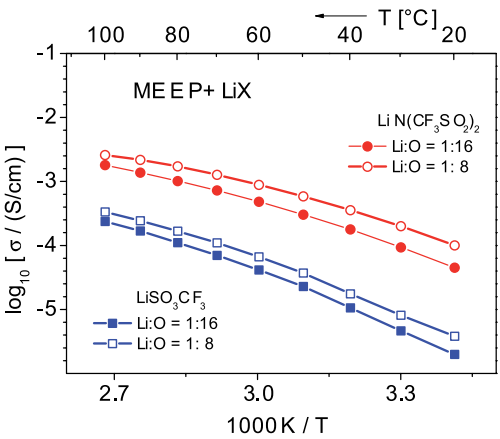

Fig. 1. Comparison of the ionic conductivities of MEEP with two different salts; the results prove a much higher dissociation of LiTFSI as compared to LiTf which explains why LiTFSI is so often used for salt-in-polymer electrolytes.

photo in Scheme 6 shows a crystalline appearance of the poly[bis-phenoxyphosphazene] (BPP), the mixed statistical substitution (1 : 1) in PMBP results in a liquid product (very low T_g), whereas the third polymer, PTFEP, is a flexible plastic polymer.

In the following, several examples will be discussed, which show the detailed influence of the substitution pattern of some polyphosphazenes on the ionic conductivity with dissolved lithium salts. The first example in Fig. 1 shows the temperature dependence of the ionic conductivity of MEEP samples which have been prepared by the living cationic polymerization [37,38]. The average molar mass was 10^5 g/mol. The polymer was a transparent highly viscous liquid. Two observations can be made: first of all, there is a clear influence of the particular choice of the anion in the lithium salt. LiTf shows almost an order of magnitude lower conductivities as compared to LiTFSI, which is explainable by the higher dissociation of LiTFSI. Second, the maximum conductivities range between 10^{-3} and 10^{-4} S/cm at room temperature for LiTFSI, which is rather high for a salt-in-polymer system. Blonsky *et al.* reported a value of 2.2×10^{-5} S/cm for a similar LiTf concentration at 30 °C which nicely agrees with Fig. 1 [6].

Figures 2 and 3 show two cases of differently substituted polyphosphazenes with a very short and a rather long sidechain. The question was: Is there a high sensitivity of the measured conductivities with respect to the length of the sidechains? Figure 2 contains conductivity data of JAPP, a polyphosphazene with long polypropylene oxide sidechains bound to the phosphorous of the polyphosphazene *via* a terminal amino group (*cf*. Scheme 5) [39]. The average molar mass of the side group alone is 500 g/mol. The conductivity is only

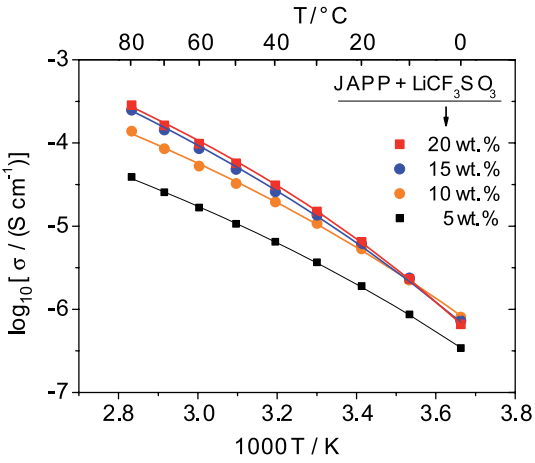

Fig. 2. Polyphosphazene functionalized with jeffamine, a molecule consisting of a long polypropylene oxide sidechain with a terminal amino group [39].

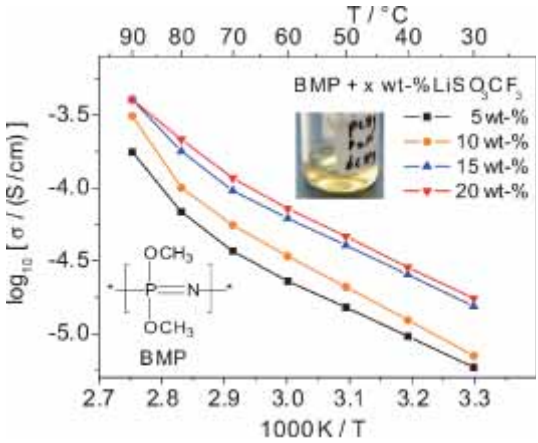

Fig. 3. Conductivity of a liquid solution of lithium triflate in poly-[bis-methoxy-phosphazene]. The glass transition temperature is rather low (−80 °C) [41].

a factor of three lower than that of MEEP (with the same lithium salt) whereas polymer electrolytes based on pure polypropylene oxide show conductivities clearly below 10^{-5} S/cm) [40]. Obviously, the high segmental mobility of the polyphosphazene backbone is favorable, as well, for an increased mobility of the attached polypropylene oxide sidechains and, hence, for the ion mobility.

BMP in Fig. 3 with the methoxy groups, on the other hand, shows one of the shortest possible functional groups at the phosphorous. The solvating capability for lithium ions may be reduced due to the lower number of donor atoms

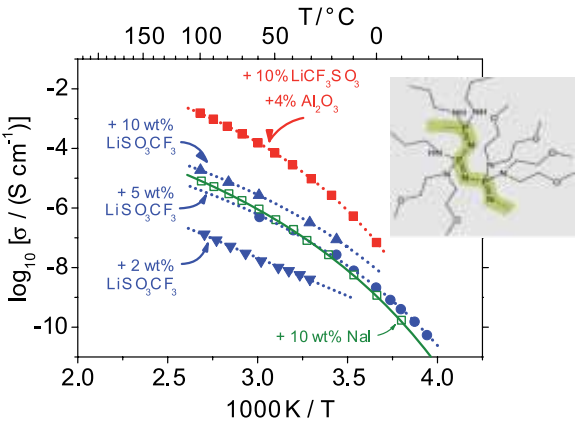

Fig. 4. Temperature dependence of the conductivities of the polymer electrolyte membranes $LiSO_3CF_3$/BMEAP, NaI/BMEAP, and $LiSO_3CF_3$/BMEAP + dispersed Al_2O_3 [38].

which may also reduce the dissociation of the salt into cations and anions. However, the mobility of the polymer segments is enhanced. SANS measurements support this: the BMP molecules in the liquid polymer behave like statistical coil molecules [41]. Therefore, it is not surprising that the conductivities of salt solutions in BMP are as high as those of MEEP with dissolved lithium triflate.

Comparing the results for the three different types of side chains of the samples in Figs. 1–3 supports the conclusion that the influence of the sidechains on the conductivities is less important than a high segmental mobility of the backbone.

Accordingly, there was hope that a branched instead of a linear sidechain would not depress the conductivity, but could help to gain mechanical stability of the salt-in-polymer solutions by chain entanglement. In order to test that, a short secondary amine with additional ether oxygen atoms was chosen for the substitution (denoted as BMEAP in Scheme 5) [38]. To guarantee a complete removal of the chlorine atoms of the precursor polymer, a primary amine was added in the final stage of the synthesis. The resulting polymer structure with a mixed substitution is illustrated in Fig. 4, too.

As expected, a considerable mechanical stability was obtained. The obtained salt-in-polymer membranes were transparent and elastic. The conductivities, however, were rather low. As can be seen in Fig. 4, the room temperature conductivity for a solution with 10 wt. % lithium triflate amounted to less than 10^{-6} S/cm. It is evident that a drastic reduction of the entire segmental motion lead to a considerable decrease of the ionic mobilities, too. Obviously, the lithium cations remain well associated within the small bags formed by the sidechains. This was confirmed by a detailed NMR analysis of the interaction between lithium ions and the BMEAP polymer [42].

It is well established from many investigations on polymer electrolytes and many other ion conducting systems that, under favorable conditions, the average ionic conductivity can considerably increase after dispersing nanoparticles within the polymer electrolyte. Since the first observations of this effect with PEO based polymer electrolytes [44], it has been intensely investigated by many authors [45–48]. Figure 4 shows the result of the dispersion of 4 wt. % Al_2O_3 nanoparticles in the LiTf/BMEAP system. The ionic conductivity at constant concentration of LiTf was increased by more than one order of magnitude. Its value at room temperature was almost comparable to the conductivity of a corresponding LiTf/MEEP solution.

Note that in conductivity studies of polymer electrolytes, the purity is an important issue. The presence of water has to be excluded by a careful choice of materials and a thorough drying process of as-prepared polymer electrolytes. The determination of remaining water is usually done by Karl-Fischer titration. Another way to determine the water content is by using NMR [49,50]. The examples presented in this overview are all characterized by careful preparation and drying processes prior to the electrochemical measurements. Details can be found in the cited publications.

2.3 Polysiloxane based electrolytes

Compared to the polyphosphazenes, the polysiloxanes possess very similar properties making them attractive for designing stable polymer electrolytes with high ionic conductivities. In particular, they exhibit high segmental mobility, good chemical stability, and like the polyphosphazenes, there is an excellent possibility to modify them with different sidechains by a universal reaction starting from poly[hydromethyl-siloxane] (PDMS) as a precursor polymer. PDMS is available as a cheap product from basic silicon chemistry. Here, PDMS was used with an average length of 35 monomer units. The Si−H groups of PDMS (*cf*. Scheme 7) were substituted *via* a platinum catalyzed hydrosilylation. It usually occurs under mild conditions and proceeds with high yield, if the introduced sidechains are not too bulky. Polysiloxanes have been prepared with different sidechains. Scheme 7 shows an example with an oligoethylene oxide. The length of the sidechains was varied over a certain range as denoted in Scheme 7, too.

Figure 5 presents temperature dependent conductivity data for two different salts dissolved in OPS(4) where (4) stands for the number of oxygen atoms in the secondary oligoether sidechains. Again, as already observed for polyphosphazenes in Fig. 1, the symmetric anion of LiBOB facilitates dissociation yielding a rather high conductivity as compared to LiTf.

A drawback of LiBOB, however, is its limited solubility (around 12 wt. %). The charge/discharge processes in a corresponding battery usually leads to a concentration gradient of the salts. Therefore, the concentration polarization during charging/discharging can cause precipitation of solid LiBOB and dam-

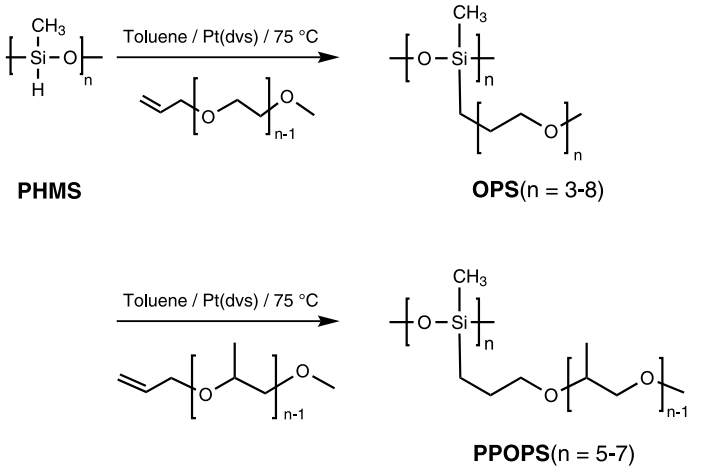

Scheme 7. Functionalization of PDMS by Pt catalyzed hydrosilylation; Pt(dvs) denotes the applied Karstedt's catalyst [43].

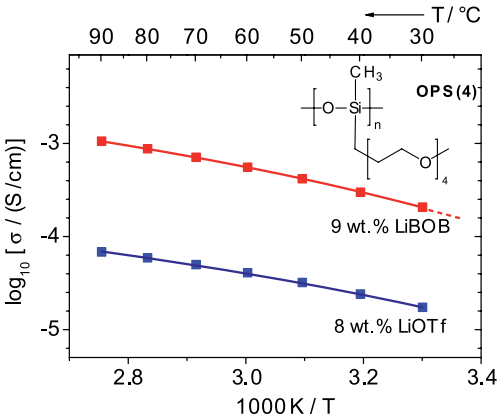

Fig. 5. Ionic conductivity of an oligoether functionalized polysiloxane with two different lithium salts (due to the higher molar mass of LiBOB, the molar concentration of LiBOB is lower by a factor of 0.68).

ages the electrode structures. Scheme 8 compiles three further substitution concepts which have been investigated within the polysiloxane class of polymer electrolytes. In most cases, maximum conductivities around 2×10^{-4} S/cm were reported [51–54].

To conclude, the ionic conductivity of salts in polyphosphazenes and polysiloxanes with ether sidechains shows maximum room temperature values around 2×10^{-4} S/cm. At present, LiTFSI seems to be the best choice in

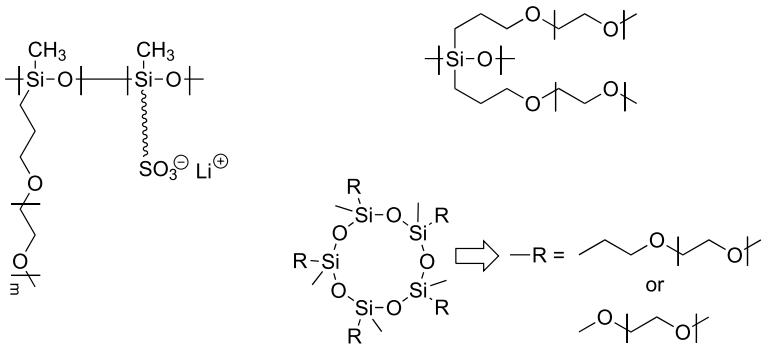

Scheme 8. Further concepts with differently functionalized polysiloxanes as published by other authors [51–54].

many cases. Nevertheless, the polysiloxanes and polyphosphazenes as described above are viscous liquids and cannot be used as dimensionally stable membranes. Obviously, in that case, one cannot speak of solid polymer electrolytes (SPE), an expression sometimes used for polymeric electrolytes. As the example BMEAP (*cf*. Fig. 3) showed, if sidechains with stronger intermolecular interactions support the formation of self-standing polymer membranes, the segmental mobility will be suppressed more or less leading to a low ion conductivity. Hence, an important task is to find a compromise between contradicting postulates, a good segmental mobility (supporting high conductivity) and a good mechanical stability. This is the topic of the following sections.

2.4 Mechanically stable polymer electrolyte membranes with high conductivity

A straightforward way to stabilize a liquid polymer and to obtain a selfstanding membrane is chemical cross-linking of the polymer molecules. There are numerous chemical reactions appropriate for that purpose. For polysiloxanes, a good approach is the sol–gel process, *i.e.* a catalyzed solvolysis of alkoxysilyl groups in the presence of water or alcohol. It is followed by a condensation reaction forming oxygen bridges between the silicon atoms of different alkoxysilyl group.

This type of reaction is also frequently used for the preparation of inorganic-organic hybrid materials, often termed as ORMOCERS (“organically modified ceramics”), where sol–gel processes are applied to couple organic molecules bearing terminal alkoxysilyl groups with hydroxo groups of *in-situ* formed silica particles [55].

ORMOCERS with dissolved salts have already been investigated as inorganic–organic hybrid electrolytes for lithium ion cells [55]. Sol gel reactions are usually carried out in the presence of acids or bases as catalysts, or

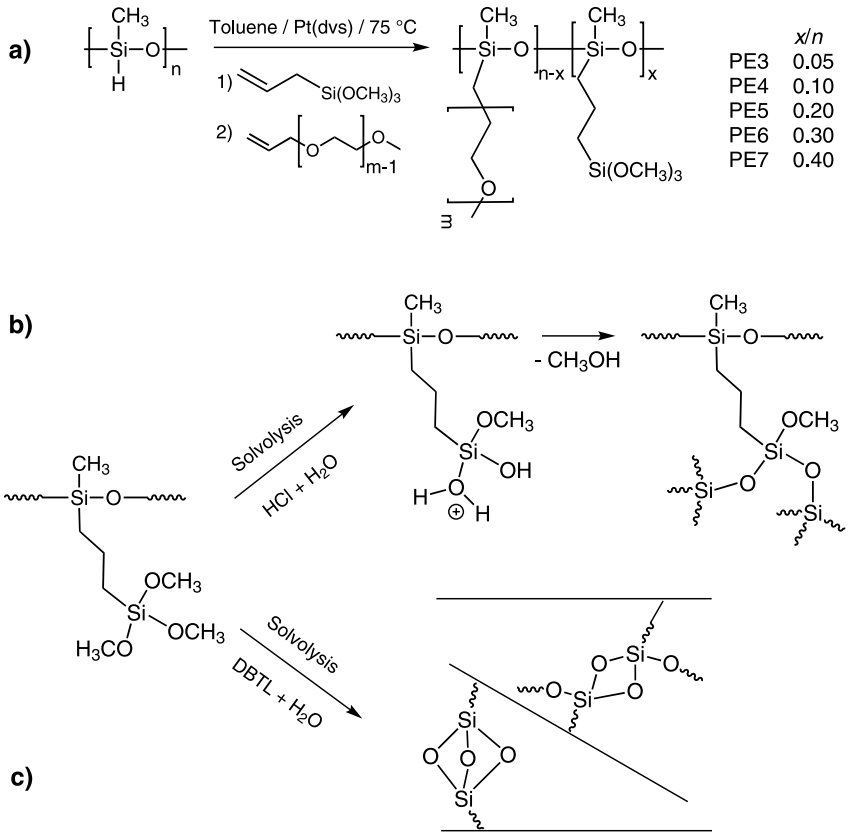

Scheme 9. a) Preparation of oligoether functionalized polysiloxanes T_xOPS with additional trimethoxysilyl groups (denoted by T) for sol–gel cross-linking [43], The chain length of the backbone was typically $n = 30$–35 (average $M_n = 2.5 \times 10^4$ g/mol, $T_g = 85$ °C). The length of the oligoether sidechain was $m = 3$–5. PE3 to PE7 denote the different cross-linker contents, **b**) cross-linking *via* acid catalyzed sol–gel process, **c**) cross-linking via a DBTL catalyzed reaction (DBTL = dibutyl tin dilaurate).

with active metal complexes as catalysts. Scheme 9 shows the reactions used to prepare cross-linked, polyether grafted polysiloxanes. It is a straightforward application of the hydrosilylation to introduce two types of sidechains for solvation of cations and for sol–gel cross-linking in a one-pot reaction.

An increasing fraction x/n of Si−O−Si bridges after cross-linking leads to a decrease of the segmental mobility and the ionic conductivity. The appearance of the polymer changes from liquid to that of a solid membrane. Hence, the percentage of cross-linking groups for a good compromise between mechanical stability and a sufficient segmental mobility had to be optimized. Figure 6 shows results for the temperature dependent ionic conductivities of

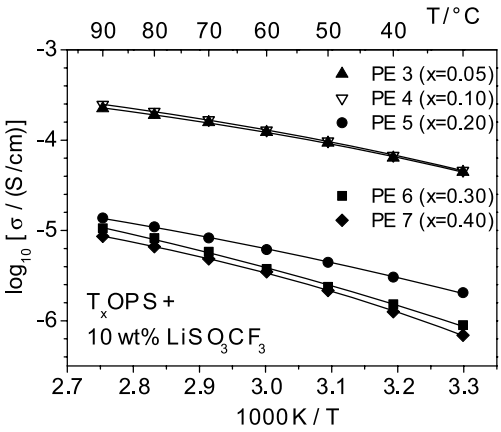

Fig. 6. Ionic conductivities of salt-in-polymer electrolyte membranes based on sol–gel cross-linked T_xOPS (HCl catalyzed) with various concentrations x of the trimethoxysilyl groups (PE3-7 denote samples with different percentages of cross-linking groups, cf. Scheme 7) [43].

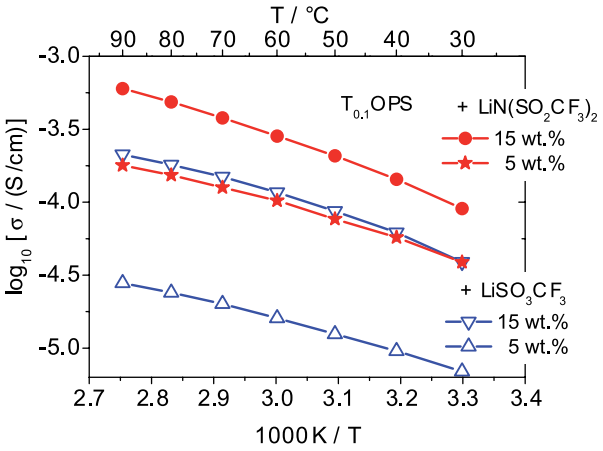

Fig. 7. Comparison of the conductivities two $T_{0.1}$OPS membranes of the same polysiloxane (HCl catalyzed) with different lithium salts [56]. As the molar mass of LiTFSI is higher compared to LiTf by a factor of 1.8, the molar concentrations of the LiTFSI solutions at the same weight percentage are a factor of about 0.5 lower.

polysiloxanes prepared with different fractions of cross-linking groups (HCl catalyzed). The general observation was that the conductivities at constant salt concentration start to decrease markedly for $x/n > 0.1$ which is obviously due to the drastic decrease of the segmental motion. Figure 7 compares the results of membranes with two different salts showing again the superior conductivity

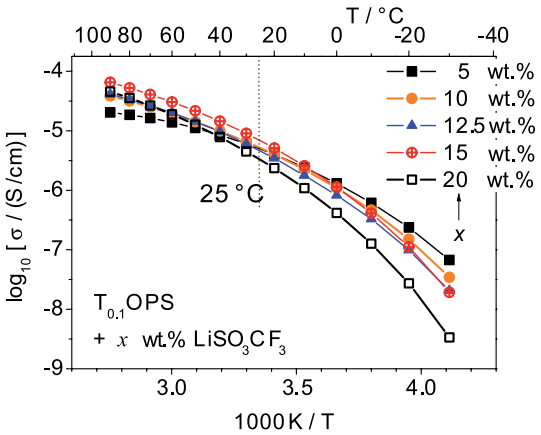

Fig. 8. DC conductivity of a $T_{0.1}$OPS membrane as a function of the LiTf concentration x (DBTL as cross-linking catalyst) [57].

with LiTFSI. In spite of the cross-linking, the conductivities are still reasonably high.

Dibutyl tin laurate (DBTL) as catalyst gave the best mechanical stability and elasticity of the membranes. This is due to the higher rate and efficiency of cross-linking (nearly 100% of the Si–OCH_3 react). It is not surprising, however, that sol–gel treated polysiloxane membranes when cross-linked with DBTL normally gave markedly lower conductivities than those cross-linked with HCl as comparison between Figs. 7 and 8 shows for the same LiTf concentration (*cf*. also data for PE 4 in Fig. 6 with the 10 wt. % sample in Fig. 8). The conductivity is lower by almost one order of magnitude.

As already mentioned in the context of the results for BMEAP (*cf*. Fig. 4), there were numerous investigations where authors tried to increase the conductivities by dispersing nanoparticles in the polymer electrolytes. In all these cases, the factors responsible for the observed increase of conductivity due to nanoparticles are well-known. A specific adsorption of anions or cations can occur at the particle surfaces depending on the Lewis acid or base character of the surface chemistry. The specific interaction leads to surface charges on the particles, increases the concentration of counterions and supports the dissociation of ion pairs in the neighbouring polymer matrix. This may then change the ionic transference numbers, too. Another well-known fact is that dispersed particles can increase the free volume in the polymer matrix around them, thus giving rise to more segmental mobility and possibly higher ionic mobility, too.

However, for polysiloxane based polymer electrolytes which already show relatively high conductivities, any further enhancement of the conductivity after adding nanoparticles is rather limited. Sometimes, one even observes a decrease as in the case of $T_{0.1}$OPS with LiTf after addition of Al_2O_3 nanopar-

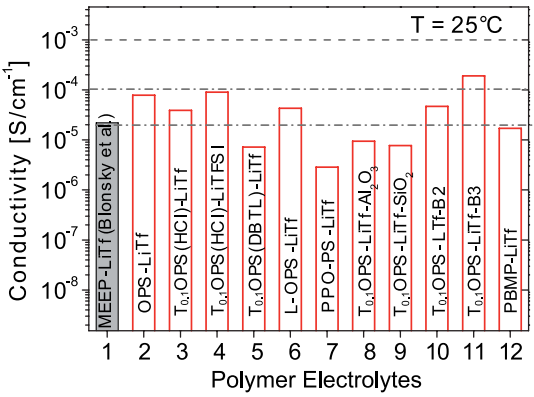

Fig. 9. Overview over the maximum room temperature conductivities of various polysiloxane based polymers [56]. The first value on the left for LiTf/MEEP is taken from the work of Blonsky *et al*. for comparison [6].

ticles [57]. To conclude this section, Fig. 9 gives an overview of the room temperature conductivities of numerous investigated salt-in-polymer electrolytes. It nicely summarizes our conclusions that the conductivities of salt-in-polymer electrolytes (without further additives except the salt!) are restricted to maximum values of around 10^{-4} S/cm as long as we speak of high molecular weight polymers ($> 10^3$ g/mol).

2.5 Extended salt-in-polymer concepts using additives and hybrid materials

The results discussed in the preceding sections make evident that an increase of the performance of non-liquid polymer electrolytes demands additional concepts beyond the simple salt-in-polymer approach which relies on amorphous low T_g polymers and salts with excellent dissociation. Therefore, it is inevitable to consider the introduction of additional components and materials that can remove the restrictions of the mere salt-in-polymer materials.

The traditional way to soften a rigid polymer network and to increase its local mobility is the addition of small molecules as plasticizers. They fill and enlarge the space between the polymer segments and lower the intermolecular interaction of the polymeric network. In the same way, such dissolved polar molecules will interact with dissolved ions and, in this way, compete with the donor atoms of the polymer chain regarding the solvation of ions. The mobility of ions in corresponding associates between ions and low molecular weight additives is considerably higher than that of ions interacting with polymer sites only. Further, the interaction of highly polar molecular additives with the salt ions will also facilitate the dissociation of more ion pairs.

One should also remember that proton conducting polymer electrolytes used for low temperature fuel cells already apply this principle for a long

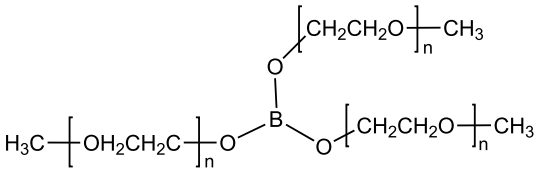

Boric acid trialkoxyesters: **B3** (n=3), **B4** (n=4)

Scheme 10. Additives based on Lewis acidic esters of boric acid which have been applied in gel polymer membranes with cross-linked polysiloxanes ($T_{0.1}$OPS) [57].

time. The proton conducting polymers usually contain a great deal of water molecules within channels of the polymer network. The water molecules act as shuttles for the transport of protons between immobile acidic sulfonate groups of the polymer network.

Accordingly, dissolving a larger concentration of small polar molecules in a salt-in-polymer electrolyte is an approach to decouple the ion transport from the slow polymer mobility and should lead to a significant increase of the conductivities This general strategy is closely connected to concepts of polymer based gel electrolytes (30 to 50 wt. % of low molecular weight components) or salt-in-polymer membranes with dissolved ionic liquids both leading to a swollen network with much higher ionic conductivity [58–62]. In order to stabilize the network it is necessary to apply cross-linking or to use polymers that favor chain entanglement.

The most simple approach is dissolve liquid aprotic polar solvents such as propylene carbonate, ethylene carbonate and others which are already well known as components of current liquid lithium battery electrolytes. But in order to develop electrolytes with higher safety, incombustible molecular additives with low volatility are preferred.

Scheme 10 shows two kind of boric ester additives with short oligoethylene oxide sidechains that were investigated as additives in cross-linked polysiloxanes [57]. Similar experiments combining related esters with other polymer electrolytes can be found in the literature [64–66]. The electron deficient boron atom acts as a Lewis acid and will therefore interact with Lewis bases and, in particular, with anions. One expects that its presence should increase the dissociation of ion pairs due to the specific interaction with the anions. Further advantages of these boron containing additives are low vapor pressure, high chemical stability, good solubility in the polymer as well as a good plasticizing function. They are available in large amounts and therefore good candidates for modified polymer electrolytes in lithium ion cells.

Figure 10 shows results for the temperature dependent conductivities of a sol–gel cross-linked polysiloxane membrane with two different boric acid ester additives. Note that the conductivity with these additives rises to values

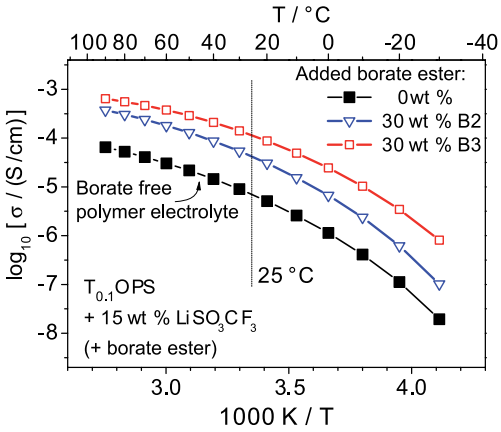

Fig. 10. Arrhenius plot of cross-linked salt-in-polysiloxane electrolytes based on $T_{0.1}$OPS with 15 wt. % lithium triflate: (a) without additives, (b) with 30 wt. % boric acid ester B2, and (c) with 30 wt. % boric acid ester B3 [57].

higher than 0.1 S/cm. Recent experiments showed that this effect may be further increased by higher amounts of the boric acid esters. Indeed, the boric acid esters themselves can be used as solvents for lithium electrolytes [67]. They are characterized by high electrochemical stability.

A further quite different concept beyond the simple salt-in-polymer approach refers back to the phosphazene derived polymers. Hexachlorocyclotriphosphazene, $(NPCl_2)_3$, is a well available industrial chemical. In close analogy to the organo substituted polyphosphazenes, one can also start $(NPCl_2)_3$ and modify this molecule by the same nucleophilic substitution reactions as used with the chlorine substituted polyphosphazene precursor (*cf*. Schemes 3 and 4). Hence, a huge variety of different organo substituted cyclic phosphazenes are obtainable. In particular, it is possible through the use of suitable sidechains to form three-dimensional networks as shown in the following. These networks can then act as hosts for incorporation of salts, plasticizers, solvents and further additives as shown in the following [18,21,63].

Scheme 11 shows three examples of synthesized cyclic triphosphazenes. The phosphorous atoms of CVEEP, CVEP and CVMEEP carry substituents with terminal vinyl groups which can be activated for a radical initiated cross-linking (*e.g.* with organic peroxides as thermally activated radical initiators). In this way, it is easy to build up a stable polymeric network from these substituted cyclic phosphazenes. One can control the rigidity and the degree of cross-linking by choosing mixed substitutions with optimized percentage of cross-linking groups (similar to the strategy applied for optimization of the T_xOPS based salt-in-polymer electrolytes, described in the preceding section). The mixed substituted CVMEEP, for instance, contains a statistical distribution

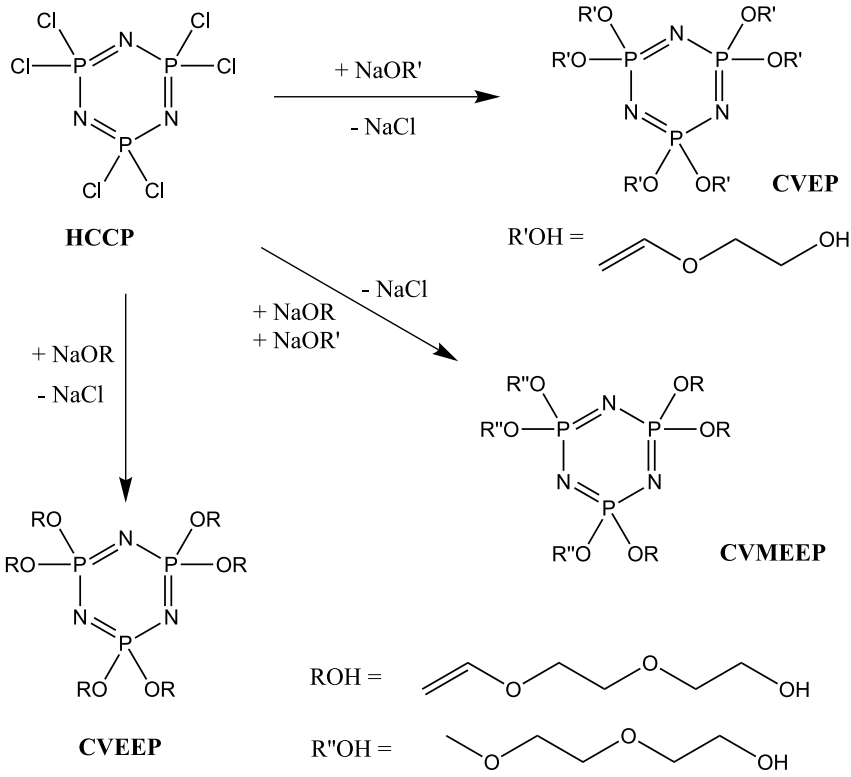

Scheme 11. Cross-linkable cyclic triphosphazenes as a different route to mechanically stable polymer electrolytes [63].

of two kinds of substituents as denoted in Scheme 11. Half of the substituents contain cross-linkable vinyl groups. The advantage of a reduced number of cross-linkable groups is that the resulting membranes are less rigid which is beneficial for the mobility of the polymeric network and, thus, of the salt ions. This was indeed verified, although the conductivities of such membranes with dissolved salt were not superior to the sol–gel cross-linked polysiloxanes (see results for CVEEP and CVEP in Figs. 11 and 12) [63].

The network resulting from cross-linking of the cyclic triphosphazenes is illustrated in Scheme 12 together with a photo of a membrane produced in this way. The procedure leads to very stable polymeric membranes. Incorporation of salts or other additives is easily possible *in-situ* during the cross-linking reaction. In parallel, Chen-Yang *et al.* developed a similar electrolyte membrane concept based on functionalized cyclic triphosphazenes [68]. An earlier work of Inoue *et al.* used a related chemistry with a graft-copolymer of polystyrene and functionlized triphosphazenes [69].

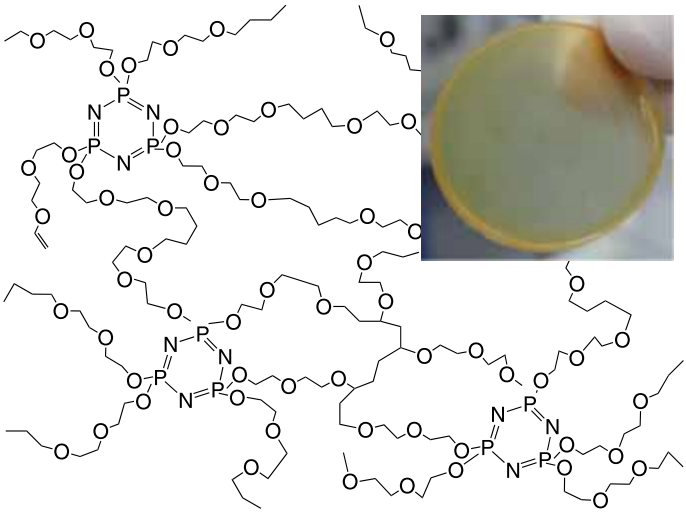

Scheme 12. Illustration of the network formed by cross-linking of CVEEP, the inserted photo gives an impression of the as-prepared membranes [63].

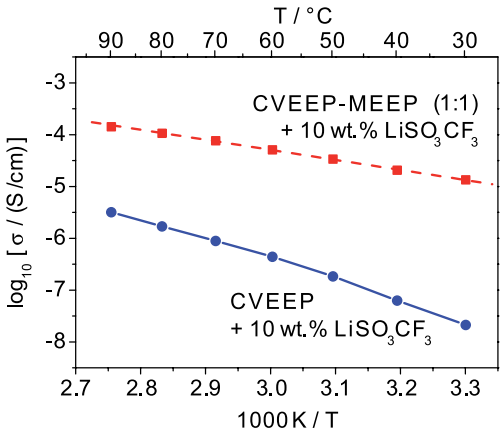

Fig. 11. Comparison of the conductivities of solutions of LiTf in a closely cross-linked CVEEP network and in a hybrid membrane containing 50% MEEP besides the network forming CVEEP [63].

Figure 11 shows the conductivity of a CVEEP membrane with LiTf. Figure 12 gives data for a CVEP membrane with LiTFSI. Again, the material with LiTFSI yields much better conductivities. However, our idea in developing these cyclomatrix networks was to apply them for a hybrid concept with liquid MEEP. As the conductivity of liquid MEEP and OPS cannot be retained after

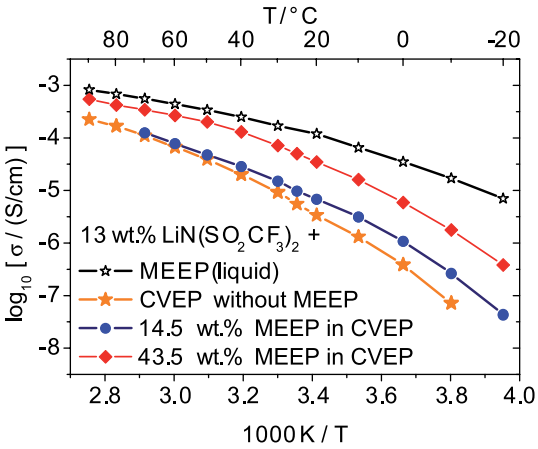

Fig. 12. Comparison of the conductivities of LiTFSI solution in the strongly cross-linked CVEP network, in liquid MEEP alone, and in hybrid materials with MEEP molecules entrapped within the CVEP network.

cross-linking, we prepared hybrid systems by confining MEEP within the cyclomatrix network of CVEEP or CVEP. Figures 11 and 12 contain results on a hybrid system consisting of the above described substituted cyclic triphosphazenes as network former and a considerable percentage of free MEEP as low T_g polymer (see formula in Scheme 5). One observes an increase of the conductivity by up to two orders of magnitude [63].

The polymer hybrid concept turns out to be an attractive idea to achieve the desired properties "high mechanical stability and high conductivity" by combining the properties of different components. MEEP induces a high local segmental mobility and thus guarantees an optimized conductivity. As Fig. 12 demonstrates, the conductivities of salt solutions in CVEP/MEEP and in pure liquid MEEP are not much different. The great advantage lies in the achieved high mechanical stability of the CVEP/MEEP hybrid membrane. This proves that dividing mechanical stability and high conductivity between two different components in a hybrid material is indeed a very good strategy.

3. Transport and electrochemistry

3.1 Mechanistic considerations and limitations of the ionic mobilities

The results in Figs. 6–8 are typical for the temperature dependence of the total conductivity of polymer electrolytes at low and medium temperatures which clearly deviates from an Arrhenius plot. Often, the empirical Vogel–Tammann–Fulcher equation (VTF equation) is used to describe and to fit the temperature

dependence of the ionic conductivity as given by

$$\sigma(T) = \frac{A_0}{T} \exp\left[\frac{-B}{T - T_0}\right] \tag{1}$$

A_0, B and T_0 are empirical constants. A consistent theoretical model to calculate these three parameters and to interpret them in terms of a transport mechanism is not available. However, a quantitative interpretation of the temperature dependent ion conductivity of polymers has been developed within the MIGRATION concept of Funke and coworkers [57,70–72]. It offers an excellent access to a quantitative description of the microscopic dynamics of ion movement in glasses and polymers. A fundamental result of the MIGRATION concept is that the conductivity σ_{DC} at low frequencies can be written as the product of the high frequency conductivity $\sigma_{HF}(T)$ and a temperature dependent function $W_\infty(T)$ according to

$$\sigma_{DC}(T) = \sigma_{HF}(T)\, W_\infty(T) \tag{2}$$

Here, $W_\infty(T)$ denotes the fraction of successful hops for a given temperature. The low frequency range used for measurements of the DC conductivity with impedance spectroscopy typically comprises 10 kHz to 0.1 Hz. Analysis of the high frequency range yields the frequency dependent complex conductivity which has been analyzed in detail for several polysiloxane based polymer electrolytes recently [57]. In molten salts and salt-in-polymer electrolytes, where the ion-sites are not predefined and where the network is not immobile, the HF conductivity is Arrhenius activated, while the DC conductivity is not. $\sigma_{HF}(T)$, accordingly it can be written as

$$\sigma_{HF}(T) = \frac{\alpha}{T} \exp\left[-\frac{E^*}{RT}\right] \tag{3}$$

Besides α, the pre-exponential factor, E^* is the activation energy required for an elementary displacive step. The model of Funke *et al.* finally yields the following temperature dependence for the DC conductivity:

$$T\sigma_{DC}(T) = \alpha \exp\left[-\frac{E^*}{RT} - \gamma \exp\left(\frac{E^*/K}{RT}\right)\right] \tag{4}$$

where in addition to the short range energy barrier E^*, the parameters γ and K determine the temperature dependence.

Figure 13 shows results of analyzing data from extended frequency dependent conductivities for cross-linked $T_{0.1}$OPS with 15 wt. % LiTf in terms of the MIGRATION model Eq. (4) [57] (same sample as in Fig. 8). The three parameters of Eq. (4) are obtained as: $E^* = 0.258$ eV, $\ln(\alpha) = 5.487$, $\gamma = 14.9 \times 10^{-3}$, and $K = 2.1$.

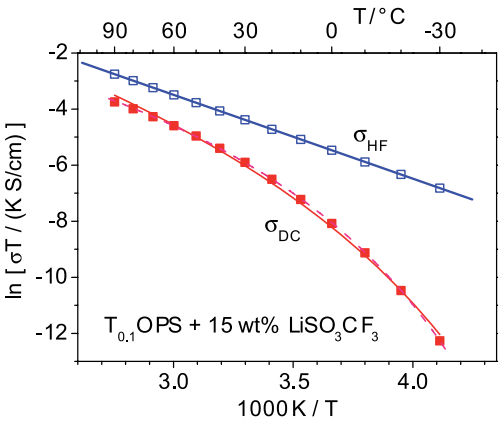

Fig. 13. Temperature dependent DC conductivity and high frequency conductivity derived from frequency dependent measurements followed by a detailed analysis using the MIGRATION concept [57].

As already mentioned, the investigations on polysiloxane and polyphosphazene based electrolytes support the conclusion that it is impossible for cross-linked salt-in-polymer membranes to achieve higher conductivities than those obtainable for the liquid polymer systems. Only an extension towards composite or hybrid systems leads to higher values by decoupling the ion mobility from the polymer. It is useful to discuss the background. The limit is caused by the restricted local thermal motion of polymer segments in polymers with high molecular weights and the absence of fast diffusion of the entire polymer molecule. As long as the mobile ions interact with the polymer network, one cannot circumvent this problem. According to Walden's rule for electrolyte solutions, the ionic mobility of liquid electrolytes is expected to change nearly proportional with the inverse of the solvent viscosity according to

$$\frac{\sigma_{\text{ion}}}{c_{\text{salt}}} \propto \frac{1}{\eta_{\text{solvent}}} \tag{5a}$$

This also holds for polymeric solvents, as long as they are amorphous, not cross-linked and their temperature is above T_g. However, an additional correction factor has to be introduced, if the salt dissociation is not complete. Nevertheless, it is useful for a rough estimate in the case of almost liquid polymers such as low T_g polysiloxanes.

Liquid hexamethyl-disiloxane, for instance, has a viscosity which is similar to that of water or propylene carbonate at ambient temperature. It is therefore not surprising that salts dissolved in tri- or tetrameric siloxanes with oligoether sidechains reach good conductivities of around 5×10^{-4} S/cm [73]. The viscosity of polymer melts scales with a power of the molar mass. Statistical

models suggest

$$\eta_{\text{polymer melt}} \propto M^p \quad \text{with} \quad p \approx 3.4 \tag{5b}$$

Hence, an increase in molar mass bei one order of magnitude from 10^2 g/mol to 10^3 g/mol should increase the viscosity by about three to four orders of magnitude, lowering the ionic mobility by a corresponding factor. A lower degree of dissociation will lead to a further decrease.

This is supported by the experiences with polyphosphazenes and polysiloxanes. Polymer electrolytes based on polysiloxanes ($M_n = (6–11) \times 10^3$ g/mol) tended to show lower viscosities than the polyphosphazenes ($M_n = 2 \times 10^4$ to 5×10^5 g/mol). Therefore, the slightly higher ionic conductivities of typical polysiloxanes (containing the same salt) can be explained by the lower molar mass. Accordingly, the conductivity of salt-in-polymer solutions can be increased using polymers with relatively low molar mass (if not cross-linked!). This is indeed the case as examples from recent publications for electrolytes with functionalized low molecular weight siloxanes show [51,54,55,73–77]. The problem of missing mechanical stability cannot be circumvented in this way. But a combination of low molecular weight solvents with cross-linked host polymer networks in hybrid membranes seems to be a promising strategy.

3.2 Ionic transference numbers

Apart from the total ionic conductivity, two further electrochemical parameters of polymer electrolytes are as important as the total conductivity for the use in lithium ion cells, *i.e.* the transference numbers of lithium ions and the electrochemical stability window. The total conductivity as measured by standard impedance spectroscopy (1–10 kHz) does not reveal the relative contribution of cations and anions to the charge transport. This information has to be determined by an independent measurement. Several techniques have been developed and published for polymer electrolytes [78–83].

The transference number of lithium ions expresses the amount of charge transport due to lithium ions under steady state conditions in lithium ion cells. If the mobilities of cations and anions of a lithium salt LiX were identical for all concentrations, the transference number should be 0.5, *i.e.* the efficiency of lithium ion transport during a steady state discharging of a lithium cell is half of that calculated from the total conductivity alone. The internal resistance is a factor of two larger than calculated from the total conductivity.

The following definition of a lithium transference number is usually found in textbooks and publications:

$$t_{\text{Li}^+} = \frac{\sigma_{\text{Li}^+}}{\sigma_{\text{Li}^+} + \sigma_{\text{X}^-}} = \frac{u_{\text{Li}^+}}{u_{\text{Li}^+} + u_{\text{X}^-}} \tag{6}$$

Local electroneutrality, *i.e.* equal local concentrations of cations and anions $c_{Li^+} = c_{X^-}$, holds in good electrolytes (except in space charge regions which are neglected here). The definition in Eq. (6) characterizes a homogeneous electrolyte as a whole. If complete dissociation of the dissolved salt LiX into Li^+ and X^- can be assumed, the ion concentrations are given by the net salt concentration, $c_{Li^+} = c_{X^-} = c_{salt}$, for incomplete dissociation $c_{Li^+} = c_{X^-} = \alpha c_{salt}$, with the degree of dissociation expressed by α. The concentration c_{LiX} of undissociated ion pairs then corresponds to $c_{LiX} = (1-\alpha)c_{salt}$.

Under charge flow, in general, a concentration gradient exists in the electrolyte. Then, the value of t_{Li^+} becomes a function of the position within the electrolyte, if the mobilities depend on the concentrations of the ions. Under these conditions, Eq. (6) is a local definition. However, for lithium ion cells, it is more interesting to describe the transference of lithium ions under the non-equilibrium conditions of steady-state charging/discharging. Corresponding experiments mostly compare the total current just after switching-on (time $t = 0$) a polarizing voltage in an initially homogeneous symmetrical cell (with the electrolyte between two Li metal electrodes) with the steady-state current reached for long times, *i.e.* $t \to \infty$. The steady-state is characterized by a vanishing anion current (if no decomposition of the electrolyte occurs) so that the total current corresponds to a net lithium ion transport.

Hence, an experimental definition of a local transference number under these conditions is:

$$t_{Li^+} = \frac{i_{tot,t\to\infty}}{i_{tot,t=0}} = \frac{(i_{Li^+})_{t\to\infty}}{(i_{Li^+} + i_{X^-})_{t=0}} \quad \text{with} \quad (i_{X^-})_{t=\infty} = 0 \tag{7}$$

where i_{tot} denotes the total electrical current density and i_{Li^+} and i_{X^-} are the partial ionic current densities of the cations and anions. t_{Li^+} becomes identical with Eq. (6) in the limit $i_{tot} \to 0$. In a charging or discharging process of a lithium ion cell, only the lithium cations take part in the electrode reactions. Under this condition, the boundary condition requires that the partial anion current density vanishes at the electrode/electrolyte interface. In the particular case of a steady state charging/discharging, this will hold throughout the entire electrolyte and implies the presence of a salt concentration gradient as shown in the following.

The general expressions for the local partial ionic current densities are

$$i_{Li^+} = -\frac{\sigma_{Li^+}}{F}\mathrm{grad}\tilde{\mu}_{Li^+}, \quad i_{X^-} = \frac{\sigma_{X^-}}{F}\mathrm{grad}\tilde{\mu}_{X^-} \tag{8}$$

F denotes Faraday's constant, $\tilde{\mu}_{Li^+}$ and $\tilde{\mu}_{X^-}$ denote the electrochemical potentials of cations and anions. Additional conditions are the expressions for the total electrical current density i_{tot} and the chemical potential of the salt μ_{LiX} given by

$$i_{tot} = i_{Li^+} + i_{X^-}, \quad \mu_{LiX} = \tilde{\mu}_{Li^+} + \tilde{\mu}_{X^-} \tag{9}$$

From the four equations in Eqs. (8) and (9), one derives

$$\begin{aligned} i_{\mathrm{Li^+}} &= -F\tilde{D}_{\mathrm{salt}}\,\mathrm{grad}\,c_{\mathrm{salt}} + t_{\mathrm{Li^+}} i_{\mathrm{tot}} \\ i_{\mathrm{X^-}} &= +F\tilde{D}_{\mathrm{salt}}\,\mathrm{grad}\,c_{\mathrm{salt}} + (1-t_{\mathrm{Li^+}}) i_{\mathrm{tot}} \end{aligned} \qquad (10)$$

$$\uparrow \qquad\qquad \uparrow$$

diffusion migration

The chemical diffusion coefficient $\tilde{D}_{\mathrm{salt}}$ of the salt (also: interdiffusion coefficient or ambipolar diffusion coefficient of the salt) in Eqs. (10) explicitly corresponds to the following expression as the derivation from Eqs. (8) and (9) shows:

$$\tilde{D}_{\mathrm{salt}} = \frac{u_{\mathrm{Li^+}} u_{\mathrm{X^-}}}{u_{\mathrm{Li^+}} + u_{\mathrm{X^-}}} \frac{RT}{F} \left(\frac{d \ln a_{\mathrm{LiX}}}{d \ln c_{\mathrm{salt}}} \right) \qquad (11)$$

As usual, the thermodynamic activity of the salt, a_{LiX}, is a function of the chemical potential μ_{LiX} of the salt according to $\mu_{\mathrm{LiX}} = \mu^{\circ}_{\mathrm{LiX}} + RT \ln a_{\mathrm{LiX}}$. where $\mu^{\circ}_{\mathrm{LiX}}$ denotes the standard value of the chemical potential. The steady-state condition of a vanishing anion current yields the following expression for the salt concentration gradient in the electrolyte:

$$\mathrm{grad}\,c_{\mathrm{salt}} = \frac{(1-t_{\mathrm{Li^+}})}{\tilde{D}_{\mathrm{salt}}} \frac{i_{\mathrm{tot}}}{F} = \frac{1}{u_{\mathrm{Li^+}}} \frac{i_{\mathrm{Li^+}}}{RT \left(\frac{d \ln a_{\mathrm{LiX}}}{d \ln c_{\mathrm{salt}}} \right)} \qquad (12)$$

if $i_{\mathrm{X^-}} = 0, i_{\mathrm{tot}} = i_{\mathrm{Li^+}}$ (steady state)

As mentioned above, one has to distinguish between the net salt concentration c_{salt} and the concentration $c_{\mathrm{LiX}} = (1-\alpha) c_{\mathrm{salt}}$ of undissociated LiX ion pairs.

In general, at high concentration gradients, ionic mobilities and transference numbers will depend on the position in the electrolyte between the electrodes. Hence, the concentration gradient, in general, will not be a linear function of the position. The calculation of an averaged transference number for higher current densities in Eq. (7) has to be done by integrating over the electrolyte thickness. Equation (8) states, as expected, that the undesired concentration polarization at high current densities is minimized by choosing an electrolyte with the highest possible lithium cation mobility, or for $t_{\mathrm{Li^+}} \to 1$.

However, the common experience with salt-in-polymer electrolytes is, if no additives or low molecular weight solvents are used, that the anion mobility is considerably higher than that of the lithium cations. Apart from that, one observes a considerable concentration of undissociated ion pairs [23,24,66,84]. The typical transference numbers of lithium ions in such salt-in-polymer electrolytes are markedly below 0.5, typically 0.2–0.3 [84]. Results obtained with pulsed field gradient NMR even showed that the diffusion of ion pairs is much higher than that of free anions and cations (*cf*. results and extended discussion

with respect to polysiloxane based electrolytes in Sect. 4 of Kunze *et al.* [24]). Under these conditions, the net lithium ion transport in the steady state may be dominated by a coupled countertransport of ion pairs and anions (which show considerably faster diffusion than the lithium cations as proved by NMR measurements for polysiloxanes [23,24] and PEO [66]). Under these conditions, mass conservation leads to the following net partial current densities of cations and anions which include the a contribution of neutral ion pairs LiX (an extended treatment of the background within the framework of irreversible thermodynamics can be found in [85,86]):

$$(i_{\mathrm{Li^+}})_{\mathrm{net}} = i_{\mathrm{Li^+}} + i_{\mathrm{LiX}},\ (i_{\mathrm{X^-}})_{\mathrm{net}} = i_{\mathrm{X^-}} - i_{\mathrm{LiX}} \qquad (13)$$

$$\text{with } i_{\mathrm{LiX}} = Fc_{\mathrm{LiX}} \frac{D_{\mathrm{LiX}}}{RT} \mathrm{grad}\, \mu_{\mathrm{LiX}}$$

The consequence of the possibility of neutral ion pair transport is to open up an additional path for a net Li^+ ion transport by a transport of LiX in one direction and a coupled transport of anions X^- in the opposite direction. Using the Eqs. (13) as a starting point, the following expressions for the transference number and for the chemical diffusion coefficient result for the transference number in electrolytes with incomplete dissociation and non-negligible fast ion pair diffusion:

$$t_{\mathrm{Li^+}} = \frac{i_{\mathrm{tot},t\to\infty}}{i_{\mathrm{tot},t=0}} = \frac{(i_{\mathrm{Li^+}})_{\mathrm{net},t\to\infty}}{(i_{\mathrm{Li^+}} + i_{\mathrm{X^-}})_{\mathrm{net},t=0}} = \frac{u_{\mathrm{Li^+}}u_{\mathrm{X^-}} + u_{\mathrm{X^-}}u_{\mathrm{LiX}} + u_{\mathrm{Li^+}}u_{\mathrm{LiX}}}{(u_{\mathrm{Li^+}} + u_{\mathrm{X^-}})\,(u_{\mathrm{LiX}} + u_{\mathrm{X^-}})} \qquad (14)$$

$$\text{with the abbreviation: } u_{\mathrm{LiX}} \equiv \frac{F}{RT} D_{\mathrm{LiX}}$$

$$\tilde{D}_{\mathrm{salt}} = \left(u_{\mathrm{LiX}} + \frac{u_{\mathrm{Li^+}}u_{\mathrm{X^-}}}{u_{\mathrm{Li^+}} + u_{\mathrm{X^-}}}\right) \frac{RT}{F} \left(\frac{d \ln a_{\mathrm{LiX}}}{d \ln c_{\mathrm{salt}}}\right) \qquad (15)$$

Equations (14) and (15) yield in the limit of a very small, negligible mobility of free lithium ions

$$t_{\mathrm{Li^+}} \approx \frac{u_{\mathrm{LiX}}}{u_{\mathrm{LiX}} + u_{\mathrm{X^-}}}, \quad \tilde{D}_{\mathrm{salt}} \approx u_{\mathrm{LiX}} \frac{RT}{F} \left(\frac{d \ln a_{\mathrm{LiX}}}{d \ln c_{\mathrm{salt}}}\right) \qquad (16)$$

$$\text{if } u_{\mathrm{Li^+}} \ll u_{\mathrm{X^-}}, u_{\mathrm{LiX}}$$

Using Eq. (16) instead of Eqs. (7) and (11) in the condition for vanishing anion current density, shows that, in principle, it seems to be an alternative solution towards fast lithium transport and high lithium transference, if a polymer with very fast diffusion of both, cation–anion pairs and free anions, could be found. This, however, has not yet been investigated.

To conclude, for estimating the properties of polymer electrolytes in a battery, the transference numbers of lithium ions have to be known. The total conductivities of amorphous salt-in-polymer electrolytes without additives

range between 10^{-4} and 10^{-5} S/cm. With transference numbers below 0.3, non-negligible concentration gradients will appear which considerably depress the efficiency of polymer electrolytes under steady-state conditions during charging/discharging. Increased salt concentration gradients in a high voltage battery may cause the risk of a serious loss of charge capacity due to precipitation of solid salt within the porous electrode structure on the high salt concentration side.

One of the most important tasks for the near future is therefore to develop composite and hybrid electrolytes with high lithium transference. Interestingly, an increase of the transference number of lithium ions has been achieved by dispersing nanoparticles, or by dissolving crown ethers or other molecules with specific ionic interactions [48,87,88]. A completely different approach was suggested and investigated by Bruce *et al.* which relies on ordered domains of PEO based electrolytes with fast transport of lithium ions along helix channels formed by the PEO backbone [89,90]. Several investigations have proved a favorable influence of ordered domains in PEO [91,92].

3.3 Stability of polymer electrolytes based on polysiloxanes and polyphosphazenes in lithium ion cells

Electrochemical stability in the potential range of interest is a required key property for a lithium battery electrolyte. The electrochemical stability is defined as the voltage range (*vs*. Li/Li^+ reference) where the electrolyte is stable *vs*. oxidation or reduction at the electrodes. Values of 4.0–4.5 V are absolutely necessary. As practically no solvent molecule is thermodynamically stable in such a large activity gradient (corresponding to 70–78 decades of the lithium activity), the materials rely on kinetic stability due to the formation of electrode/electrolyte interlayers (SEI = solid/electrolyte interphase) or simply on metastability and slow reaction kinetics. One of the future strategies to achieve higher energy densities in lithium batteries aims at even higher cell voltages. Hence, development of novel solvents, lithium salts and additives with enhanced high voltage stability is an important task.

The electrochemical stability of the organo-functionalized polysiloxanes and polyphosphazenes was investigated under the conditions of lithium cells. A conventional closed three electrode cell was used consisting of an inert working electrode (Ni, Pt) according to

$$\text{Li}|\text{electrolyte membrane}|\text{Ni (or Pt)} \tag{10}$$

Metallic lithium was applied as material for the counter and reference electrodes. The polymer electrolyte was measured in the form of a cross-linked elastic membrane with a thickness around or below 100 μm. The interface between the electrolyte membrane and the electrodes was kept under light pressure by spring loading. Several different materials were tested as working

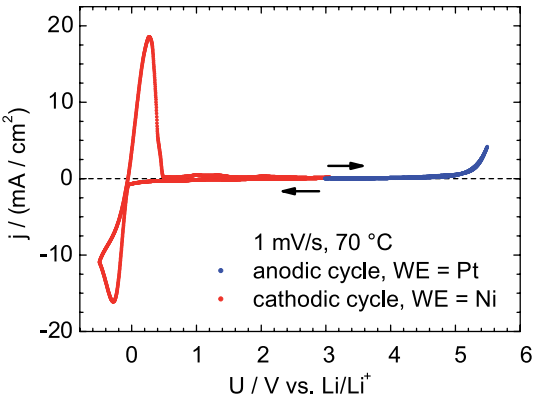

Fig. 14. Cyclic voltammetry of a polysiloxane membrane, $T_{0.1}$OPS, containing 0.6 mmol/$g_{polymer}$ LiBOB (cross-linked with $Si(OMe)_3$-sidegroups in 10% of the monomeric siloxane units).

electrodes. The final materials were chosen in order to minimize any corrosion or dissolution of the working electrode during the experiments. Cyclic voltammetry curves were taken at 70 °C in order to minimize the electrolyte resistance.

Figure 14 shows a typical curve of cyclic voltammetry at 70 °C for a polysiloxane based membrane with dissolved LiBOB (*cf*. Scheme 2). It is contains separate voltage scans in the high and the low potential range, each one starting at a medium potential near 3 V (*vs*. Li/Li^+). As the chemical diffusion coefficients of the salts within the polymer are low, the sweep rates were kept small. The peaks around 0 V in Fig. 14 are caused by lithium plating on nickel. The reverse peaks near 0 V show the re-dissolution of lithium ions into the electrolyte. Anodic oxidation sets in at about 4.6 V accompanied by exponential current increase for potentials larger than 5 V. This reaction is due to the oxidation of the oligoether sidechains and is in agreement with results of other authors for PEO and graft-copolymers of PEO with other backbones. As can be inferred from Fig. 14, polysiloxane based electrolytes are stable with the currently used lithium anode and cathode materials (*e.g.* $LiFePO_4$: 3.3–3.6 V).

Figure 15 shows corresponding results for a polymer electrolyte made from a cross-linked MEEP membrane. In this example, LiDFOB was the dissolved salt (*cf*. structure of LiDFOB in Scheme 2). It becomes evident that the oxidation limit of the MEEP membrane extends to even higher potential values as compared to the polysiloxane. This observation was valid for all comparable experiments with polysiloxanes and polyphosphazenes. Thus, one can conclude that the oxidation of the sidechains at the polyphosphazenes is more hindered and slower. It is not easy to explain that as the oligomeric ether sidechains were the same. Possibly, the oxidation products at the interface form a better stabilizing film with polyphosphazene than with polysiloxane.

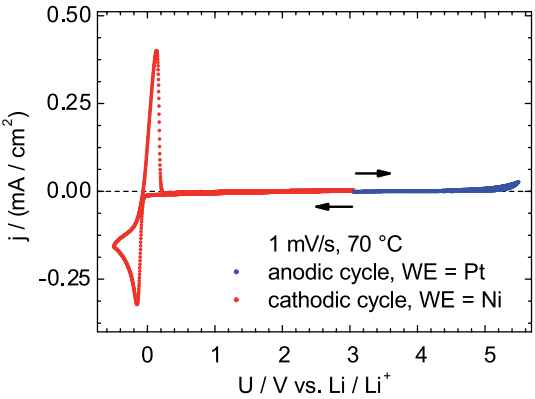

Fig. 15. Cyclic voltammetry of a polyphosphazene membrane (MEEP) containing 0.8 mmol/$g_{polymer}$ LiDFOB (cross-linked with the help of 5 wt. % benzophenone activated by UV irradiation).

The peaks at the low potential end of the voltage scale around 0 V in Fig. 15 are sharper, because the membrane thickness and therefore also the polymer electrolyte resistance were rather small as compared to the polysiloxane in Fig. 14. Both examples in Figs. 14 and 15 give a clear statement that the electrochemical stability of polysiloxanes and polyphosphazenes is suitable for an application in lithium batteries. At present, an increasing number of experimental results are available which prove that hybrid or gel type electrolytes prepared with polyphosphazenes and polysiloxanes can attain sufficient ionic conductivities with the help of low molecular weight additives and show excellent cycling stability. They are easily produced as thin films with excellent adhesion on the current anode and cathode materials of lithium cells.

4. Final remarks

One of the conclusions of the research on polyphosphazenes and polysiloxanes is that the intrinsic limitations of ionic transport due to coupling to the polymer mobility limits the conductivities at room temperature to values around 0.1 mS/cm or only slightly higher. For liquid polysiloxanes and polyphosphazenes with low T_g, a possibility exists to reduce the viscosity by choosing rather low molar masses (significantly below 10^3 g/mol). Of course, the consequence is that one leaves the field of polymers. In order to use the advantage of polymer chemistry with respect to mechanical stability and safety, the necessarily enhanced intermolecular interaction or cross-linking inevitably slows down the molecular mobility and with it the ion mobility. Nevertheless, as the results described in this article showed, electrolytes made of cross-linked polymer membranes can be optimized by making use of composite and hy-

brid concepts. The dispersion of nanoparticles alone is not enough to achieve conductivities and ion mobilities as those found in liquid electrolytes. But, incorporation of low molecular weight additives has a great influence and can decouple the ion transport from the polymer network in the background. In this context, concepts of nano- or micro-structured polymer networks such as foams or ordered pore channels become quite interesting if combined with a low viscosity additive. To conclude, polymer based electrolyte concepts remain attractive for application in batteries. There is a good perspective that suitable electrolytes will be designed for the next generation of lithium batteries.

Acknowledgement

This work was part of the research program A2 within the collaborative research center "SFB 458", funded by the Deutsche Forschungsgemeinschaft. We thank K. Funke, R. Banhatti, H. Eckert, C. Cramer-Kellers, M. Schönhoff, A. Heuer, R. Pöttgen, B. Krebs, T. Nilges, N. Stolwijk, L. van Wüllen and D. Wilmer for helpful discussions, thanks also to all colleagues in the SFB 458 for the excellent collaboration. Finally, we would like to acknowledge the collaboration with D. Richter, R. Zorn, and W. Pyckhout-Hintzen on SANS experiments in Jülich, the collaboration with S. Passerini and M. Winter regarding the electrochemical analysis of polymer electrolytes in lithium ion cells, and we thank H. Gores (University Regensburg) and G. Röschenthaler (Jacobs University Bremen) for preparing and making available a number of novel lithium salts.

References

1. D. E. Fenton, J. M. Parker, and P. V. Wright, Polymer **14** (1973) 589.
2. M. B. Armand, J. M. Chabagno, and M. J. Duclot, in: Second International Meeting on Solid Electrolytes, St. Andrews, Scotland (1978).
3. B. L. Papke, R. Dupon, M. A. Ratner, and D. F. Shriver, Solid State Ion. **5** (1981) 685.
4. M. Armand, Solid State Ion. **9**/**10** (1983) 745.
5. P. M. Blonsky, D. F. Shriver, P. Austin, and H. R. Allcock, J. Am. Chem. Soc. **106** (1984) 6854.
6. P. M. Blonsky, D. F. Shriver, P. Austin, and H. R. Allcock, Solid State Ion. **18**/**19** (1986) 258.
7. J. S. Tonge, P. M. Blonsky, D. F. Shriver, H. R. Allcock, P. E. Austin, T. X. Neenan, and J. T. Sisko, J. Electrochem. Soc. **133** (1986) C293.
8. D. Fish, I. M. Khan, and J. Smid, Makromol. Chem.-Rapid Commun. **7** (1986) 115.
9. J. Smid, D. Fish, I. M. Khan, E. Wu, and G. B. Zhou, Adv. Chem. Ser. (1990) 113.
10. J. B. Goodenough and Y. Kim, Chem. Mater. **22** (2010) 587.
11. J. W. Fergus, J. Power Sources **195** (2010) 4554.
12. J. B. Kerr, in: *Lithium Batteries – Science and Technology*, G. Nazri and G. Pistoia (eds.), Kluwer Academic Publishers, Boston (2004), p. 574.
13. F. Gray and M. Armand, in *Handbook of Battery Materials*, J. O. Besenhard (ed.), Wiley-VCH, Weinheim, New York (1999).

14. W. H. Meyer, Adv. Mater. **10** (1998) 439.
15. G. X. Wang, L. Yang, Y. Chen, J. Z. Wang, S. Bewlay, and H. K. Liu, Electrochim. Acta **50** (2005) 4649.
16. Y. H. Huang, K. S. Park, and J. B. Goodenough, J. Electrochem. Soc. **153** (2006) A2282.
17. A. Fedorkova, R. Orinakova, A. Orinak, I. Talian, A. Heile, H. D. Wiemhöfer, D. Kaniansky, and H. F. Arlinghaus, J. Power Sources **195** (2010) 3907.
18. M. Burjanadze, J. Paulsdorf, N. Kaskhedikar, Y. Karatas, and H. D. Wiemhöfer, Solid State Ion. **177** (2006) 2425.
19. M. Burjanadze, PhD Thesis, WWU, Münster, (2006).
20. Y. Akgöl, C. Hofmann, Y. Karatas, C. Cramer, H. D. Wiemhöfer, and M. Schönhoff, J. Phys. Chem. B **111** (2007) 8532.
21. H. R. Allcock, *Chemistry and Applications of Polyphosphazenes*, John Wiley & Sons, New Jersey (2003).
22. R. G. Jones, W. Ando, and J. Chojnowski, *Silicon-Containing Polymers – The Science and Technology of Their Synthesis and Applications (Chapt. 1–3)*, Kluwer Academic Publ., Dordrecht, Boston, London (2000), p. 768.
23. M. Kunze, Y. Karatas, H. D. Wiemhöfer, H. Eckert, and M. Schönhoff, Phys. Chem. Chem. Phys. **12** (2010) 6844.
24. M. Kunze, A. Schulz, H.-D. Wiemhöfer, H. Eckert, and M. Schönhoff, Z. Phys. Chem. **224** (2010).
25. R. J. Klein, D. T. Welna, A. L. Weikel, H. R. Allcock, and J. Runt, Macromolecules **40** (2007) 3990.
26. E. S. Peterson, T. A. Luther, M. K. Harrup, J. R. Klaehn, M. L. Stone, C. J. Orme, and F. F. Stewart, J. Inorg. Organomet. Polym. Mater. **17** (2007) 361.
27. H. R. Allcock, J. M. Nelson, S. D. Reeves, C. H. Honeyman, and I. Manners, Macromolecules **30** (1997) 50.
28. H. R. Allcock, S. D. Reeves, C. R. de Denus, and C. A. Crane, Macromolecules **34** (2001) 748.
29. H. R. Allcock and R. L. Kugel, Inorg. Chem. **5** (1966) 1016.
30. G. Dhalluin, R. Dejaeger, J. P. Chambrette, and P. Potin, Macromolecules **25** (1992) 1254.
31. T. Kinoshita, Y. Ogata, M. Suzue, and T. Hasegawa, Japanese Patent, JP 55043174 (1980).
32. K. Matyjaszewski, M. K. Moore, and M. L. White, Macromolecules **26** (1993) 6741.
33. C. H. Honeyman, I. Manners, C. T. Morrissey, and H. R. Allcock, J. Am. Chem. Soc. **117** (1995) 7035.
34. J. M. Nelson, H. R. Allcock, and I. Manners, Macromolecules **30** (1997) 3191.
35. B. Wang, E. Rivard, and I. Manners, Inorg. Chem. **41** (2002) 1690.
36. B. Wang, Macromolecules **38** (2005) 643.
37. J. Paulsdorf, M. Burjanadze, K. Hagelschur, and H. D. Wiemhöfer, Solid State Ion. **169** (2004) 25.
38. J. Paulsdorf, N. Kaskhedikar, M. Burjanadze, S. Obeidi, N. A. Stolwijk, D. Wilmer, and H. D. Wiemhöfer, Chem. Mater. **18** (2006) 1281.
39. N. Kaskhedikar, J. Paulsdorf, M. Burjanadze, Y. Karatas, D. Wilmer, B. Roling, and H. D. Wiemhöfer, Solid State Ion. **177** (2006) 703.
40. M. M. Doeff, P. Georen, J. Qiao, J. Kerr, and L. C. De Jonghe, J. Electrochem. Soc. **146** (1999) 2024.
41. Y. Karatas, W. Pyckhout-Hintzen, R. Zorn, D. Richter, and H. D. Wiemhöfer, Macromolecules **41** (2008) 2212.
42. L. van Wüllen, T. K. J. Köster, H. D. Wiemhöfer, and N. Kaskhedikar, Chem. Mater. **20** (2008) 7399.

43. Y. Karatas, N. Kaskhedikar, M. Burjanadze, and H. D. Wiemhöfer, Macromol. Chem. Phys. **207** (2006) 419.
44. J. E. Weston and B. C. H. Steele, Solid State Ion. **7** (1982) 75.
45. S. Jung, D. W. Kim, S. D. Lee, M. Cheong, D. Q. Nguyen, B. W. Cho, and H. S. Kim, Bull. Korean Chem. Soc. **30** (2009) 2355.
46. A. M. Stephan and K. S. Nahm, Polymer **47** (2006) 5952.
47. M. Ciosek, L. Sannier, M. Siekierski, D. Golodnitsky, E. Peled, B. Scrosati, S. Glowinkowski, and W. Wieczorek, Electrochim. Acta **53** (2007) 1409.
48. H. Mazor, D. Golodnitsky, Y. Rosenberg, E. Peled, W. Wieczorek, and B. Scrosati, Isr. J. Chem. **48** (2008) 259.
49. M. Amereller, M. Multerer, C. Schreiner, J. Lodermeyer, A. Schmid, J. Barthel, and H. J. Gores, J. Chem. Eng. Data **54** (2009) 468.
50. H. G. Schweiger, M. Multerer, U. Wietelmann, J. C. Panitz, T. Burgemeister, and H. J. Gores, J. Electrochem. Soc. **152** (2005) A622.
51. R. Hooper, L. J. Lyons, M. K. Mapes, D. Schumacher, D. A. Moline, and R. West, Macromolecules **34** (2001) 931.
52. G. B. Zhou, I. M. Khan, and J. Smid, Macromolecules **26** (1993) 2202.
53. D. P. Siska and D. F. Shriver, Chem. Mater. **13** (2001) 4698.
54. Z. C. Zhang, L. J. Lyons, J. J. Jin, K. Amine, and R. West, Chem. Mater. **17** (2005) 5646.
55. M. Popall, R. Buestrich, G. Semrau, G. Eichinger, M. Andrei, W. O. Parker, S. Skaarup, and K. West, Electrochim. Acta **46** (2001) 1499.
56. Y. Karatas, PhD Thesis, WWU, Münster, Germany (2006).
57. Y. Karatas, R. D. Banhatti, N. Kaskhedikar, M. Burjanadze, K. Funke, and H. D. Wiemhöfer, J. Phys. Chem. B **113** (2009) 15473.
58. M. Morita and N. Yoshimoto, in *Advanced Materials and Methods for Lithium-Ion Batteries*, S. S. Zhang (ed.), Transworld Research Network, Trivandrum, Kerala (2007), p. 321.
59. A. M. Stephan, Eur. Polym. J. **42** (2006) 21.
60. P. L. Kuo, S. S. Hou, C. Y. Lin, C. C. Chen, and T. C. Wen, J. Polym. Sci. Pol. Chem. **42** (2004) 2051.
61. G. T. Kim, G. B. Appetecchi, M. Carewska, M. Joost, A. Balducci, M. Winter, and S. Passerini, J. Power Sources **195** (2010) 6130.
62. J. Rymarczyk, M. Carewska, G. B. Appetecchi, D. Zane, F. Alessandrini, and S. Passerini, Eur. Polym. J. **44** (2008) 2153.
63. N. Kaskhedikar, M. Burjanadze, Y. Karatas, and H. D. Wiemhöfer, Solid State Ion. **177** (2006) 3129.
64. Y. Kato, S. Yokoyama, T. Yabe, H. Ikuta, Y. Uchimoto, and M. Wakihara, Electrochim. Acta **50** (2004) 281.
65. E. Zygadlo-Monikowska, Z. Florjanczyk, A. Tomaszewska, M. Pawlicka, N. Langwald, R. Kovarsky, H. Mazor, D. Golodnitsky, and E. Peled, Electrochim. Acta **53** (2007) 1481.
66. F. Kaneko, S. Wada, M. Nakayama, M. Wakihara, and S. Kuroki, Chem. Phys. Chem. **10** (2009) 1911.
67. Y. Tanaka, J. Kaneko, M. Minoshima, Y. Iriyama, and T. Fujinami, Electrochemistry **78** (2010) 397.
68. Y. W. Chen-Yang, S. Y. Chen, C. Y. Yuan, C. H. Tsai, and D. P. Yan, Macromolecules **38** (2005) 2710.
69. K. Inoue, K. Takiue, and T. Tanigaki, J. Polym. Sci. Pol. Chem. **34** (1996) 1331.
70. K. Funke, R. D. Banhatti, D. Laughman, M. Mutke, and M. D. Ingram, Eur. Phys. J.-Spec. Top. **161** (2008) 65.
71. S. J. Pas, M. D. Ingram, K. Funke, and A. J. Hill, Electrochim. Acta **50** (2005) 3955.
72. S. J. Pas, R. D. Banhatti, and K. Funke, Solid State Ion. **177** (2006) 3135.

73. N. A. A. Rossi, Z. C. Zhang, Y. Schneider, K. Morcom, L. J. Lyons, Q. Z. Wang, K. Amine, and R. West, Chem. Mater. **18** (2006) 1289.
74. L. Z. Zhang, Z. C. Zhang, S. Harring, M. Straughan, R. Butorac, Z. H. Chen, L. Lyons, K. Amine, and R. West, J. Mater. Chem. **18** (2008) 3713.
75. Z. C. Zhang, L. J. Lyons, K. Amine, and R. West, Macromolecules **38** (2005) 5714.
76. B. Oh, D. Vissers, Z. Zhang, R. West, H. Tsukamoto, and K. Amine, J. Power Sources **119** (2003) 442.
77. S. Skaarup, K. West, B. Zachau-Christiansen, M. Popall, J. Kappel, J. Kron, G. Eichinger, and G. Semrau, Electrochim. Acta **43** (1998) 1589.
78. H. Hafezi, and J. Newman, J. Electrochem. Soc. **147** (2000) 3036.
79. Y. P. Ma, M. Doyle, T. F. Fuller, M. M. Doeff, L. C. Dejonghe, and J. Newman, J. Electrochem. Soc. **142** (1995) 1859.
80. J. Evans, C. A. Vincent, and P. G. Bruce, Polymer **28** (1987) 2324.
81. P. G. Bruce and C. A. Vincent, J. Electroanal. Chem. **225** (1987) 1.
82. L. Niedzicki, M. Kasprzyk, K. Kuziak, G. Z. Zukowska, M. Armand, M. Bukowska, M. Marcinek, P. Szczecinski, and W. Wieczorek, J. Power Sources **192** (2009) 612.
83. M. Ciosek, M. Marcinek, G. Zukowska, and W. Wieczorek, Electrochim. Acta **54** (2009) 4487.
84. N. Kaskhedikar, J. Paulsdorf, A. Burjanadze, Y. Karatas, B. Roling, and H. D. Wiemhöfer, Solid State Ion. **177** (2006) 2699.
85. J. Maier and G. Schwitzgebel, Phys. Status Solidi b **113** (1982) 535.
86. H. D. Wiemhöfer, Solid State Ion. **40**(1) (1990) 530.
87. D. Golodnitsky, R. Kovarsky, H. Mazor, Y. Rosenberg, I. Lapides, E. Peled, W. Wieczorek, A. Plewa, M. Siekierski, M. Kalita, L. Settimi, B. Scrosati, and L. G. Scanlon, J. Electrochem. Soc. **154** (2007) A547.
88. A. Blazejczyk, W. Wieczorek, R. Kovarsky, D. Golodnitsky, E. Peled, L. G. Scanlon, G. B. Appetecchi, and B. Scrosati, J. Electrochem. Soc. **151** (2004) A1762.
89. E. Staunton, Y. G. Andreev, and P. G. Bruce, Faraday Discuss. **134** (2007) 143.
90. A. M. Christie, S. J. Lilley, E. Staunton, Y. G. Andreev, and P. G. Bruce, Nature **433** (2005) 50.
91. L. Gitelman, M. Israeli, A. Averbuch, M. Nathan, Z. Schuss, and D. Golodnitsky, J. Comput. Phys. **227** (2008) 8437.
92. D. Golodnitsky and E. Peled, Electrochim. Acta **45** (2000) 1431.